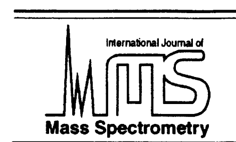

International Journal of Mass Spectrometry 194 (2000) 269–288

Characterisation of product ions in high-energy tandem mass spectra of protonated oligonucleotides formed by electrospray ionisation

Allan Weimann[1], Paula Iannitti-Tito[2], Margaret M. Sheil*

Department of Chemistry, University of Wollongong, NSW 2522, Australia

Received 6 September 1999; accepted 13 September 1999

Abstract

Tandem mass spectra of positively charged ions of a range of small oligonucleotides (6–10 mers) have been examined in detail using a hybrid magnetic sector time-of-flight mass spectrometer. This has a higher range of collision energies (up to E_{lab}400 eV) and a different timescale of dissociation compared to triple quadrupole and quadrupole ion trap instruments. Under these conditions loss of neutral guanine and cytosine bases is frequently observed and this results in additional product ions comprising strands of the phosphodiester backbone with only 1–3 bases (especially adenine and thymine) attached. The relative abundance of ions from the bases (BH_2^+) and ions from loss of a neutral base with the chain remaining intact also do not follow a clear trend in contrast to previous studies on triple quadrupoles, except that a protonated base ion derived from thymine is never observed. The relative abundance of the remaining BH_2^+ ions varied with both oligonucleotide sequence and the charge on the precursor, suggesting that under the collision conditions employed, the relative proton affinities of the bases adenine, cytosine, and guanine are not the only factors influencing ion abundance. For two of the oligonucleotides, 5′-CACGTG-3′ and 5′-CGTACG-3′, all of the fragment ions were also generated via collisional activation in the source and their tandem mass spectra examined to assist in the identification of the product ions observed in the tandem mass spectra of the intact oligonucleotides. These data also provide new information concerning the mechanisms by which oligonucleotides fragment in the positive ion mode. For example, the ion at *m/z* 81, which has been alternatively attributed to either a phosphate ion or to a sugar ion, is shown here to be derived principally from the sugar. This suggests that the sugar residues rather than the phosphate backbone are the most likely site of protonation after the nucleobases. Finally, tandem mass spectra of selected $[M + H]^+$ and $[M + 2H]^{2+}$ precursors have been compared to the tandem mass spectra of the corresponding $[M - H]^-$ and $[M - 2H]^{2-}$ ions obtained under the same collision conditions. In the case of singly charged precursors, the formation of singly charged sequence ions is equally constrained by the fact that loss of neutral thymine is strongly disfavoured and consequently the sequence ions (w_n and a_n-B_n) observed in each case are similar. In contrast, for the doubly charged precursors there are marked differences in the relative abundance of these sequence ions because loss of thymine as an anion to yield singly charged sequence ions is possible for the deprotonated $[M - 2H]^{2-}$ precursors whereas the analogous pathway from the doubly protonated precursors is clearly unfavourable. (Int J Mass Spectrom 194 (2000) 269–288) © 2000 Elsevier Science B.V.

Keywords: Electrospray ionisation; Matrix-assisted laser desorption ionisation; Protonated oligonucleotides; Quadrupole ion trap; Tandem mass spectrometry

* Corresponding author. E-mail: Margaret_Sheil@uow.edu.au

[1]Current address: Copenhagen University Hospital Q7642, Tagensvej 20, DK-2200 Copenhagen, Denmark.

[2]Current address: Oxford Centre for Molecular Sciences, South Parks Rd., Oxford, OX1 3QT, UK.

Dedicated to Professor J. Morrison on the occasion of his 75th birthday in recognition of his distinguished contributions to mass spectrometry.

1387-3806/00/$20.00 © 2000 Elsevier Science B.V. All rights reserved

PII S1387-3806(99)00236-5

1. Introduction

Following the introduction of electrospray ionisation (ESI) and matrix-assisted laser desorption ionisation (MALDI), the use of mass spectrometry for the characterisation of nucleic acids and nucleic acid constituents has expanded rapidly. This has encom-

passed a wide variety of different applications including sequencing modified and unmodified oligonucleotides (using either ESI tandem mass spectrometry or a combination of enzymatic digests with MALDI), characterisation of antisense oligonucleotides, ribonucleotides, and ligand–oligonucleotide adducts [1,2].

There have also been a relatively large number of studies aimed at describing the fragmentation of oligonucleotide anions in the gas phase [3–12]. In contrast, the fragmentation of positively charged oligonucleotides has received less attention [13–15]. The preference for analysis of oligonucleotides in the negative ion mode stems largely from the fact that in solution the phosphate backbone is deprotonated and thus negatively charged. Furthermore, tandem mass spectra of multiply charged anions have been shown to yield superior sequence information compared to the corresponding spectra obtained in the positive ion mode. This is largely because in positive ion tandem mass spectra, the 3′ sequence ions (i.e. w ions according to the nomenclature introduced by McLuckey [3]) to the 3′ side of thymine are normally not present, whereas in negative ion tandem mass spectra the full w series is usually present and can be recognised on the basis of peak height.

Positive ion spectra can, however, give valuable information, especially when characterising modifications in DNA. For example, if a species has been formed via adduction with metal complexes or alkylating agents, which naturally carry one or more positive charges, small fragments containing the modification will not easily accommodate a net negative charge, whereas they will readily carry a net positive charge. This is borne out in the studies of platinated oligonucleotide adducts which have shown that positive ion tandem mass spectra yield the most useful structural information [16]. McCloskey and co-workers have also highlighted other potential advantages of studying positive ion spectra of oligonucleotides [14]. First, positive ion spectra of oligonucleotides generally show fewer charge states than the corresponding negative ion spectra [13–15]. This may simplify interpretation of spectra when the mass difference between the oligonucleotides is small (e.g. when distinguishing between C versus U in RNA for high values of z). For short oligonucleotides, the ion yields may also be higher in the positive ion mode, thus affording better sensitivity. Hence, positive ion analysis of oligonucleotides may find applications where sensitivity and simplicity of the resulting spectra are prime considerations.

Preliminary investigations of ESI tandem mass spectra of protonated oligonucleotides have been reported by Ni et al. [14] who examined a range of doubly charged tetramers. They found that the primary fragmentation pathway observed for protonated oligonucleotides was similar to that observed for deprotonated oligonucleotides, i.e. charged base loss followed by cleavage of the C–3′–O–3′ phosphodiester bond. The ion abundances for loss of protonated bases corresponded with measured proton affinities of the bases (C $>$ G $>$ A $\gg$ T) with protonation of thymine being strongly disfavoured. The abundance of w and a-B sequence ions resulting from cleavage of the ribose 3′–C–O bond correlated with the proton affinities of the base to the 5′ side of the cleavage site. The w and a-B sequence ions where the base to the 5′ side of the cleavage site was a thymine were absent. Loss of terminal bases, in particular the 3′-terminal base was favoured over loss of internal bases.

In a separate article that appeared at the same time, Wang et al. [15] investigated the fragmentation of protonated and deprotonated oligonucleotides up to 20 bases in length. Base composition was found to influence the charge state distribution of protonated oligonucleotide molecular ions in ESI mass spectra, with T-containing sequences yielding lower average charge states. Consistent with the results of Ni et al. [14], the tandem mass spectra in both ionisation modes yielded similar product ions, with w and a-B sequence ion formation in the positive ion mode enabling sequence determination. These workers also observed the absence of w and a-B sequence ions in the tandem mass spectrum of a protonated oligonucleotide comprising only the thymine base. The presence of relatively abundant series of x and z sequence ions, and the lack of protonated thymine was proposed to be a consequence of the site of protonation

being at the 5′-phosphodiester oxygen rather than on the nucleobases.

A significant amount of work has also been conducted on the fragmentation of positively charged dinucleotides. Phillips and McCloskey [17] investigated the low energy fast-atom bombardment (FAB) tandem mass spectra of both protonated and deprotonated species of all possible heterogenous-base sequences of 2′ deoxyribonucleotides and ribonucleotides. These workers derived gas-phase structures of both protonated and deprotonated dinucleotide ions demonstrating the factors contributing to stabilisation of the tertiary structure such as intramolecular hydrogen bonding and charge delocalisation effects. These structures were proposed as models to rationalise the observed dissociation products. In the fragmentation of protonated oligonucleotides, the tertiary dinucleotide structure involved the bases sharing the proton from ionisation. They found that the product ion for the 3′ base was always more abundant than the 5′ base (except when thymine is the 3′ base). This was attributed to interaction between the phosphate and the 3′ base, which induces a partial positive charge on the 3′ base, and enhances glycosidic bond cleavage. The results obtained in our laboratory for ESI tandem mass spectrometry of a range of dinucleotides [18] were consistent with the FAB tandem mass spectrometry results of Phillips and McCloskey [17].

Rodgers et al. have also undertaken similar studies on protonated dinucleotides using a Fourier transform mass spectrometry (FT-MS) instrument [19]. Their results were in good agreement with those of Phillips and McCloskey [17]. Protonated base loss was proposed to occur via a multicentered elimination mechanism. The site of protonation on the base directs elimination of the protonated base as a stable tautomer. Upon base elimination, it was proposed that an intermediate hydrogen-bound complex is formed between the base and the complementary fragment. Competitive dissociation of this complex can generate either the protonated base or the dinucleotide product ion resulting from neutral base loss. The observed effect of thymine loss being disfavoured was rationalised first on the basis of its substantially lower proton affinity relative to the other bases. This agreed with their estimates of the relative proton affinities of the bases that followed the order C > G > A > T with the values for the proton affinities of C, G, and A within a similar range [19]. Secondly, calculated energies of the most stable tautomeric forms of each of the nucleobases upon elimination as a neutral tautomer, BH, showed that the next most stable tautomeric forms of cytosine and guanine in comparison to the most common tautomers were 0.6 kcal mol^{-1} and 1.5 kcal mol^{-1} higher in energy, whereas with adenine the energy difference was 6.7 kcal mol^{-1} and for thymine 9.0 kcal mol^{-1}. Therefore they proposed that thymine is a much less stable leaving group compared to the other bases.

In this article we examine the tandem mass spectra of singly and doubly protonated ions from intact oligonucleotides and the tandem mass spectra of the product ions generated in the ion source. The abundance of sequence ions and ions owing to charged bases in positive ion spectra for different oligonucleotide sequences are compared. This article emphasises detailed characterisation of the product ions and aims to give a better understanding of the major fragmentation pathways of positively charged oligonucleotides rather than exploring the potential of this technique for sequencing oligonucleotides. Further, the effect of using a higher range of collision energies (up to 400 eV) than is typically employed in triple quadrupole experiments is considered.

2. Experimental

2.1. Oligonucleotide preparation and purification

Synthetic oligonucleotides were obtained from Auspep Pty. Ltd., Victoria, Australia in the trityl-on form, attached to the controlled pore gas (CPG) solid support column. Deprotection, cleavage, and reversed-phase high-performance liquid chromatography (HPLC) purification of the oligonucleotides was carried out using methods described previously [20].

2.2. Mass spectrometry

A VG Autospec orthogonal acceleration time-of-flight (oa-TOF) magnetic sector mass spectrometer (Wythenshawe, England) equipped with an electrospray ion source was employed in the current study. This instrument comprises a magnetic sector of *EBE* configuration as MS1 and an oa-TOF analyser as MS2. A detailed description of the instrument is given elsewhere [21]. Oligonucleotide samples were prepared for MS analysis by dissolving the dried oligonucleotide in water and diluting to yield 50 pmol/μL of single stranded oligonucleotide in an aqueous solution of 50% 2-propanol and 1% acetic acid. The solutions were introduced into the electrospray source by continuous infusion via a Harvard Apparatus (South Natick, MA) syringe pump at a flow rate of 5 μL/min. The voltage on the electrospray probe tip was between 3–4 kV with 0.5 kV on the counter electrode. Solvent evaporation was aided through the use of a countercurrent flow of nitrogen and a nebuliser gas (concurrent flow of nitrogen) was employed to assist in stabilizing the spray.

2.3. Tandem mass spectrometry

Positive ion tandem mass spectra were acquired for the $[M + H]^+$ ions of the sequences 5′-CACGTG-3′, 5′-CGTACG-3′, 5′-ATGCAT-3′, 5′-CGGCCG-3′, and the $[M + 2H]^{2+}$ ions for the oligonucleotides 5′-CGTACG-3′, 5′-CGGCCG-3′, 5′-CGGTACCG-3′, 5′-GCGTACGC-3′, and 5′-GGTAATTACC-3′. In addition, negative ion tandem mass spectra were acquired on $[M - H]^-$ ions of 5′-ATGCAT-3′ and $[M - 2H]^{2-}$ ions of 5′-CACGTG-3′ and 5′-CGT ACG-3′, respectively, for comparison. A collision cell voltage of 400 V was used for singly charged ions and 200 V for the doubly charged ions. Methane was employed as the collision gas [21]. For each sample the pressure of the gas in the collision cell was adjusted to obtain an optimum amount of information in both the low and high mass ranges. All tandem mass spectra were acquired over the range of *m/z* 1–3500.

Tandem mass spectra were also acquired for the all of the product ions observed in the tandem mass spectra of the $[M + H]^+$ precursor ions of both 5′-CACGTG-3′ and 5′-CGTACG-3′. The product ions were generated in the source by adjusting the voltages on the sampling cone and skimmer lens. The ion of interest was then selected in MS1 (the magnetic sector), collisionally activated in the collision cell, and the product ion spectrum was recorded in MS2, i.e. the oa-TOF.

3. Results

3.1. Tandem mass spectra of singly charged ions

Fig. 1 shows the tandem mass spectra of the $[M + H]^+$ ions of 5′-CACGTG-3′. The nomenclature used here for the assignment of the product ions is a variation on the nomenclature of McLuckey et al. [3], whereby the oligonucleotide is considered to be a neutral species and the additional hydrogens gained or lost on cleavage are specified as summarised in Table 1. The identities of all the product ions in the tandem mass spectra of 5′-CACGTG-3′ were assigned based on tandem mass spectra of the corresponding product ions generated by collisional activation in the source (as discussed in more detail below). The most abundant product ion in the spectrum is $[sA - H_2O) + H]^+$ (*m/z* 216) and there are abundant ions owing to $[A_{nt} + s + p + H]^+$ (*m/z* 492), and the sequence ions $[w_2 + 2H]^+$ (*m/z* 652) and $[w_3 + 2H]^+$ (*m/z* 981). There are also relatively weak $[w_4 + 2H]^+$ (*m/z* 1270) and $[w_5 + 2H]^+$ (*m/z* 1583) sequence ions. The $[a_2 - B_2H]^+$ (*m/z* 388), $[a_3 - B_3H]^+$ (*m/z* 701), and $[a_4 - B_4H]^+$ (*m/z* 990) ions are also present as relatively abundant ions. The $[w_1 + 2H]^+$ and $[a_5 - B_5H]^+$ sequence ions, both of which would arise following loss of thymine, are absent from the spectrum. There are also ions owing to loss of neutral guanine (*m/z* 1642) and cytosine (*m/z* 1681). In the low *m/z* region of the spectrum there are BH_2^+ ions from guanine (*m/z* 152), adenine (*m/z* 136), and cytosine (*m/z* 112) and an abundant ion at *m/z* 81 that we show here arises from the sugar (more below). The remaining ions in the spectrum arise from strings of

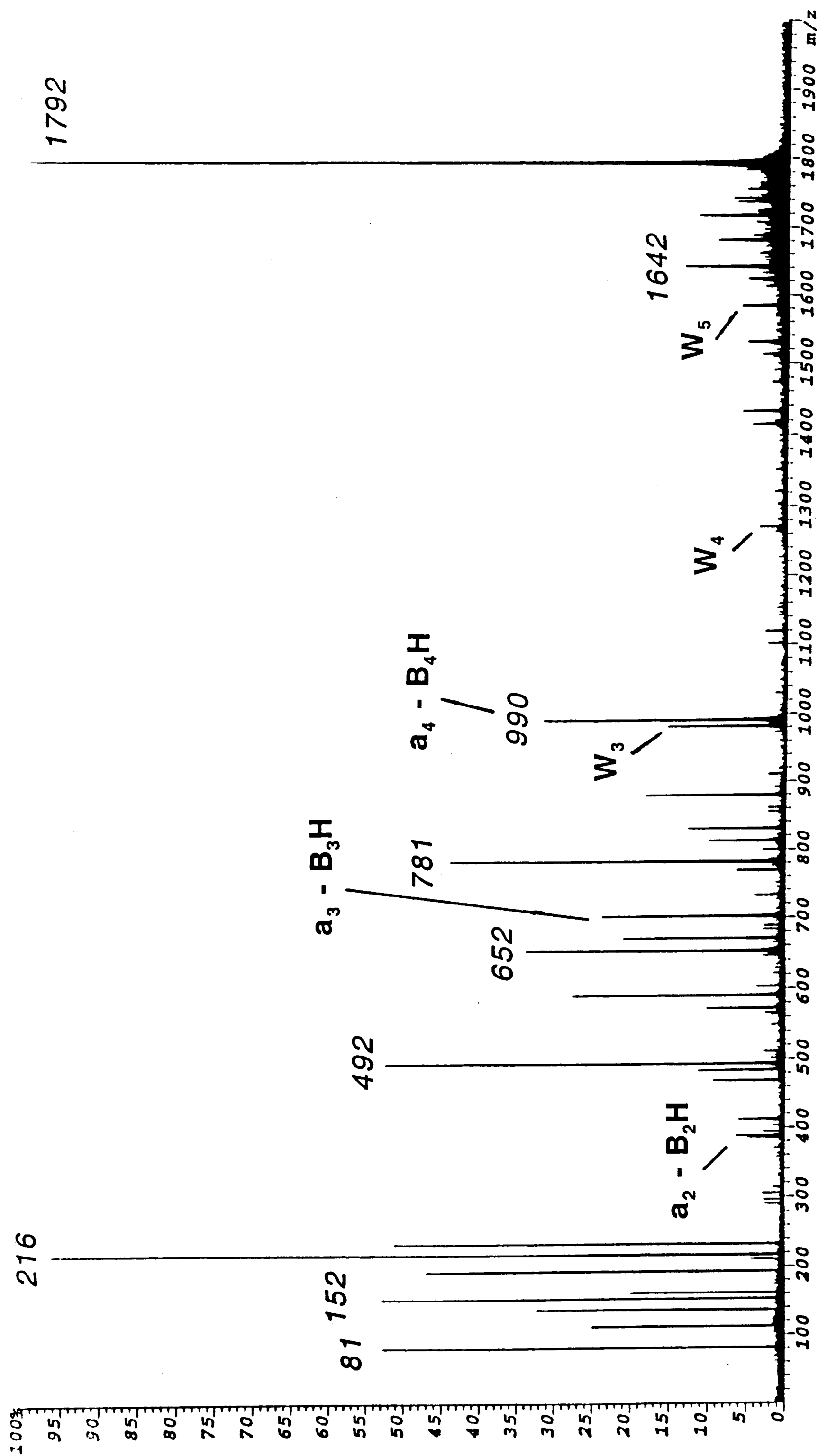

Fig. 1. Tandem mass spectrum of the $[M + H]^+$ ion (m/z 1792) of 5′-CACGTG-3′.

Table 1
Net hydrogen transfer associated with formation of positively charged sequence ions

Cleavage type	Singly charged cations	Multiply charged cations[a]
5′ Sequence ions		
a	a^+	$[\{a + (n - 1)H\}/n]^{n+}$
a − BH	$[a - BH]^+$	$[\{a + (n - 1)H\text{-}BH\}/n]^{n+}$
b	$[b + 2H]^+$	$[\{b + (n + 1)H\}/n]^{n+}$
c	c^+	$[\{c + (n - 1)H\}/n]^{n+}$
d	$[d + 2H]^+$	$[\{d + (n + 1)H\}/n]^{n+}$
3′ Sequence ions		
w	$[w + 2H]^+$	$[\{w + (n + 1)H\}/n]^{n+}$
x	x^+	$[\{x + (n - 1)H\}/n]^{n+}$
y	$[y + 2H]^+$	$[\{y + (n + 1)H\}/n]^{n+}$
z	z^+	$[\{z + (n - 1)H\}/n]^{n+}$

[a] Where n is the number of charges.

backbone containing various combinations of sugar and phosphate residues and one to three bases as shown in Table 2. It appears that the majority of these strings of backbone ions result from loss of G and C bases because combinations containing AC or GT, with the neighbouring bases being C and G, are the most abundant of these series in the spectrum of 5′-CACGTG-3′ and TA-, TAC-, or GTA-containing fragments are the most abundant in the spectrum of 5′-CGTACG-3′.

Table 3 shows the major w and a-B sequence ions and the relative abundance of the ions owing to the protonated bases and ions formed by loss of a neutral base where the chain remains intact in the tandem

Table 2
Common low *m/z*, nucleotide, and polynucleotide ions observed in tandem mass of positively charged oligonucleotides

Backbone fragment ions[a]	*m/z*
$[s - H_2O + H]^+$	81
$[p + s - H_2O + H]^+$	161

Nucleoside and base ions	*m/z*
$[CH_2]^+$	112
$[AH_2]^+$	136
$[GH_2]^+$	152
$[sC - H_2O + H]^+$	192
$[sC + H]^+$	210
$[sA - H_2O + H]^+$	216
$[sG - H_2O + H]^+$	232

Mononucleotide ions X =	C	T	A	G
X_{nt}	290	305		
X_{nt} + p or +(s − H_2O)		385	394	
X_{nt} + s or + (p + H_2O)	388	403		
X_{nt} + p + s	468	483	492	

	5′-CACGTG-3′			5′-CGTACG-3′		
Backbone ions	A_{nt}	(CA)	(GT)	(TA)	(TAC)	(GTA)
		603		618		
+p or + (s − H_2O)	412	683				
+s or + (p + H_2O)		701	732	716	1005	
+p + s	492	781	812	796	1086	1124
+p + s + H_2O	510	799			1103	1143
+p + s + p or +s + p + s − H_2O	572	861	892	876	1223	
+p + s + p + H_2O or +s + p + s	590	879	910	894	1183	
+p + s + p + s − H_2O	652				1281	
+p + s + p + s	670			974		
+p + s + p + s + p + H_2O or + s + p + s + p + s	768			993		

[a] Where $p = PO_3H$, s = deoxyribose-H_2O ($C_5H_6O_2$).

Table 3
Comparison of relative intensities of major ions in MS/MS spectra of positively charged oligonucleotides

Precursor	BH_2^+	Loss of BH	w_n ions: Most abundant	w_n ions: Absent	$[a_n - B_nH]^+$
$[M + H]^+$					
5′CACGTG3′	G > A > C	G > C	$[w_2 + H]^+$, $[w_3 + H]^+$	w_1	$[a_4 - B_4H]^+ > [a_3 - B_3H]^+ > [a_2 - B_2H]^+$
5′CGTACG3′	A > G > C	G > C	$[w_2 + H]^+$, $[w_4 + H]^+$	w_3	$[a_2 - B_2H]^+ \sim [a_5 - B_5H]^+ > [a_4 - B_4H]^+$
5′ATGCAT3′	A > C > G	—	$[w_2 + H]^+$, $[w_3 + H]^+$	w_1, w_4	$[a_3 - B_3H]^+ > [a_4 - B_4H]^+ > [a_5 - B_5H]^+$
5′CGGCCG3′	C > G	—	$[w_2 + H]^+$, $[w_3 + H]^+$	w_5	$[a_3 - B_3H]^+ > [a_2 - B_2H]^+$
$[M + 2H]^{2+}$					
5′CGTACG3′	G > C > A	C > G	$[w_1 + 2H]^+$, $[w_5 + 3H]^{2+}$	w_3	$[a_3 - B_3H]^+ \sim [a_2 - B_2H]^+$
5′CGGCCG3′	G > C	C > G	$[w_1 + 2H]^+$, $[w_5 + 3H]^{2+}$		$[a_4 - B_4H]^+ > [a_3 - B_3H]^+ > [a_2 - B_2H]^+$
5′GCGTACGC3′	C > G > A	G > C ≫ A	$[w_1 + 2H]^+$, $[w_7 + 3H]^{2+}$	w_4	$[a_3 - B_3H]^+ > [a_2 - B_2H]^+$
5′CGGTACCG3′	C > G > A	G > C ≫ A	$[w_1 + 2H]^+$, $[w_6 + 3H]^{2+}$, $[w_7 + 3H]^{2+}$	w_4	$[a_3 - B_3H]^+ \gg [a_4 - B_4H]^+ \sim [a_5 - B_5H]^{\sim}[a_6 - B_6H]^+$
5′GGTAATTACC3′	G > C > A	G > C ≈ A	$[w_1 + 2H]^+$, $[w_9 + 3H]^{2+}$	w_4, w_5	$[a_2 - B_2H]^+ \gg [a_4 - B_4H]^+ \sim [a_5 - B_5H]$

mass spectra of $[M + H]^+$ precursors of 5′-CACGTG-3′, 5′-CGTACG-3′, 5′-ATGCAT-3′, and 5′-CGGCCG-3′. Considering first the abundance of the BH_2^+ ions, apart from the absence of ions owing to protonated thymine (consistent with its significantly lower proton affinity), there is no clear trend to account for the abundance of the remaining base ions. This suggests that in the case of C, A, and G, where the differences in proton affinities are small, other factors such as the stabilities of the resulting product ions, the effect of sequence variations, and the possibility of multiple collisions may be more significant under the collision conditions employed here.

The influence of base composition is more evident when considering the ions arising from loss of a neutral base when the chain remains intact. For these ions, loss of GH and, to a slightly lesser extent, CH are favoured in all the examples, apart from the spectrum of 5′-ATGCAT-3′. In the latter case the presence of an ion owing to loss of AH may be a consequence of the adenine being located at the 5′ terminus. Alternatively, the fact that this oligonucleotide contains two adenines may simply increase the probability of the adenine bases being lost as a neutral with the chain remaining intact. There were no ions arising from loss of the neutral bases with the chain remaining intact in the spectrum of 5′-CGGCCG-3′, suggesting that this oligonucleotide is more susceptible to subsequent fragmentation. The absence of ions owing to the loss of TH, and the fact that loss of AH is not always observed, may be a consequence of the comparatively lower stability of the major tautomeric forms making these less favourable leaving groups than GH and CH, as described by Rodgers [19].

In the case of both the w-type and a-B sequence ions, the most abundant ions are those arising from loss of GH, and to a lesser extent CH. Sequence ions resulting from loss of adenine were generally of much lower abundance and those from loss of thymine were completely absent from these spectra. There is also a close correlation between the relative abundance of the w and a-B ions. For example, in the case of 5′-CACGTG-3′, the $[w_2 + 2H]^+$ and $[a_4 - B_4H]^+$ ions resulting from loss of the G-4 are the most abundant ions in their respective series. Similarly, the

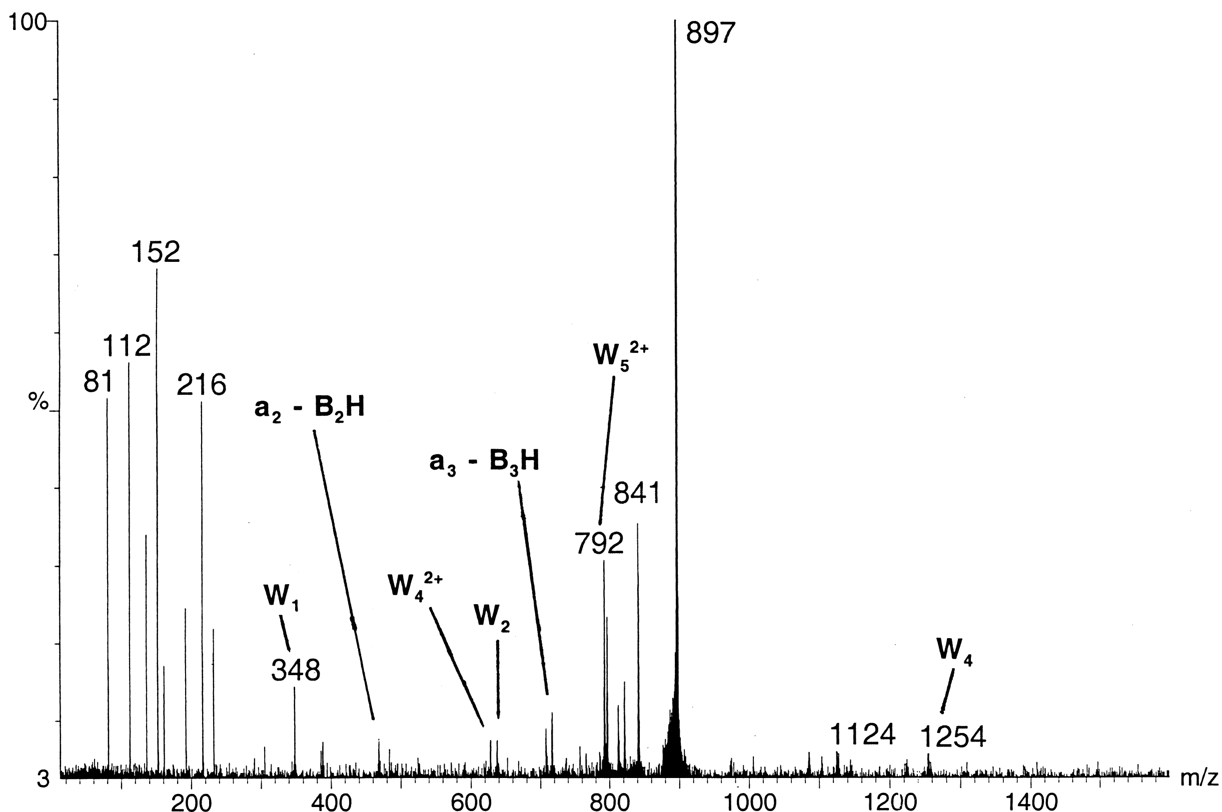

Fig. 2. Tandem mass spectrum of the $[M + 2H]^{2+}$ ion (*m/z* 897) of 5′-CGTACG-3′.

$[w_4 + 2H]^+$ and $[a_2 - B_2H]^+$ ions resulting from loss of G-2 are the most abundant in each series in the spectrum of 5′-CGTACG-3′.

3.2. Tandem mass spectra of doubly charged ions

Fig. 2 shows the tandem mass spectra of the $[M + 2H]^{2+}$ ion of 5′-CGTACG-3′. The tandem mass spectrum of the $[M + H]^+$ precursor (not shown) contained a series of sequence ions (apart from those that would follow loss of thymine) and the strings of backbone ions that were evident in the spectrum of 5′-CACGTG-3′ (Fig. 1). As with 5′-CACGTG-3′, all product ions were also generated via collisional activation in the ESI source and their tandem mass spectra were used to assign the identities of the ions in the tandem mass spectrum. There are abundant peaks in the spectrum arising from the BH_2^+ ions of the bases (with that from guanine being the most abundant and there being no base ion from thymine), the $[sA - H_2O) + H]^+$ ion (*m/z* 216), and various other sugar, phosphate combinations.

The tandem mass spectrum of the $[M + 2H]^{2+}$ ion (Fig. 2) also shows the $[w_1 + 2H]^+$ (*m/z* 348), $[w_2 + 2H]^+$ (*m/z* 637), $[w_4 + 2H]^+$ (*m/z* 1254), $[w_4 + 3H]^{2+}$ (*m/z* 628), and $[w_5 + 3H]^{2+}$ (*m/z* 792) ions. There is no w_3 ion, which would arise following the loss of thymine and the $[a_n - B_nH]^+$ ions are generally absent or of very low abundance apart from the $[a_3 - B_3H]^+$ ion at *m/z* 716.7 and $[a_2 - B_2H]^+$ *m/z* 388. There are abundant doubly charged ions arising from loss of CH (*m/z* 841) and GH (*m/z* 821). There are several peaks comprising strings of backbone, i.e. $[GTA + s + p + H]^+$ at *m/z* 1085 and [TA + s +

p + H]$^+$ at *m/z* 812, but in general these ions were less abundant in the spectra of the doubly charged precursors compared to the singly charged precursors. Another interesting difference between the spectra of the [M + H]$^+$ and [M + 2H]$^{2+}$ ions 5′-CGTACG-3′ is that the abundance of the BH_2^+ ions are: G > C > A in the spectrum of the doubly charged precursor (Fig. 2) and A > G > C for the singly charged (more below).

The spectra of the [M + 2H]$^{2+}$ ions of the other oligonucleotides examined (not shown) were qualitatively very similar to that of 5′-CGTACG-3′. Similar trends were evident, i.e. the backbone ions were relatively less abundant; not all the w sequence ions were observed; and the a − B_n ions were of lower abundance than in the spectra of the corresponding singly charged precursors. Table 3 shows the major sequence ions and order of relative abundance of base ions. In contrast to the spectra of the singly charged precursors, where the most abundant w ions were generally w_2, w_3, or w_4, depending on the position and identities of the bases, the most abundant w ions in the spectra of the [M + 2H]$^{2+}$ precursors are those arising following loss of the 5′ base that yields either w_9, w_7, or w_5 (depending on the length of the oligonucleotide) and the w_1 ions from loss of the base once removed from the 3′ terminus. This is consistent with the most probable sites of protonation being on the central bases in the case of singly protonated oligonucleotides, and on the terminal bases in the doubly charged precursors. The latter is not unexpected given that this would minimise Coulombic repulsion in the precursor ions.

With regard to the abundance of the BH_2^+ ions, it is difficult to establish a clear trend from the data obtained here. In the spectrum of the [M + H]$^+$ ion of 5′-ATGCAT-3′, the BH_2^+ ion from A is much more abundant than the corresponding ions derived from C and G. In the tandem mass spectra of the [M + 2H]$^{2+}$ ions from 5′-CGGTACCG-3′ and 5′-GCGTACGC-3′, the order of abundance of BH_2^+ ions is C > G ≫ A. It is also interesting to note that in the spectrum of the [M + H]$^+$ ion of 5′-CGGCCG-3′, CH_2^+ yields the most abundant base ion, whereas in the spectrum of the [M + 2H]$^{2+}$ ion, the GH_2^+ ion is the most abundant, which again suggests that differences in the most probable sites of protonation may affect the relative abundance of these ions. The site(s) of protonation are likely to be determined by a combination of the effects of Coulombic repulsion and the relative proton affinity of the bases. For example, in the case of 5′-CGTACG-3′, the BH_2^+ from A-4 is most abundant in the spectrum of the [M + H]$^+$ ions, whereas the BH_2^+ from either G-2 or G-6 (or both) is the most abundant ion in the spectrum of the [M + 2H]$^{2+}$ ions. Furthermore, under the conditions employed here the ions will experience multiple collisions without the aid of collision damping as occurs in, say, a quadrupole ion trap. Hence the stability of the product ions is also likely to be a major factor in determining relative ion abundance.

3.3. Comparison of tandem mass spectra of protonated and deprotonated oligonucleotides

The tandem mass spectra of the [M + H]$^+$ and [M − H]$^-$ precursor ions of 5′-ATGCAT-3′ shown in Fig. 3 are remarkably similar. In the spectrum of the protonated precursor [Fig. 3(a)] the most abundant ion is the BH_2^+ ion from adenine (*m/z* 136) and there are relatively abundant [w_2 + 2H]$^+$ (*m/z* 637) and [w_3 + 2H]$^+$ (*m/z* 925) ions and a weak [w_5 + 2H]$^+$ (*m/z* 1558) ion. The [w_4 + 2H]$^+$ ion that would arise following loss of thymine is absent from the spectrum. The [a_3 − B_3H]$^+$ (*m/z* 716), [a_4 − B_4H]$^+$ (*m/z* 1045), and [a_5 − B_5H]$^+$ (*m/z* 1335) ions are evident in the spectrum. Loss of neutral guanine (*m/z* 1640), adenine (*m/z* 1656), and cytosine (*m/z* 1681) are also present in relatively low abundance. In the low *m/z* region there are also ions for the bases (apart from thymine), and nucleoside and mononucleotide ions including *m/z* 207 and *m/z* 305 from T-containing fragments. There are also a series of backbone ions, the most abundant being [TA − p − s + H_2O + H]$^+$ *m/z* 814.

In the spectrum of the [M − H]$^-$ ion [Fig. 3(b)] the relative abundance of the sequence ions follow the same trends as the [M + H]$^+$ ions, i.e. w_3^- (*m/z* 923) > w_2^- (*m/z* 634) ≫ w_5^- (*m/z* 1556). There are abundant ions owing to [a_4 − B_4H − 2H]$^-$ (*m/z*

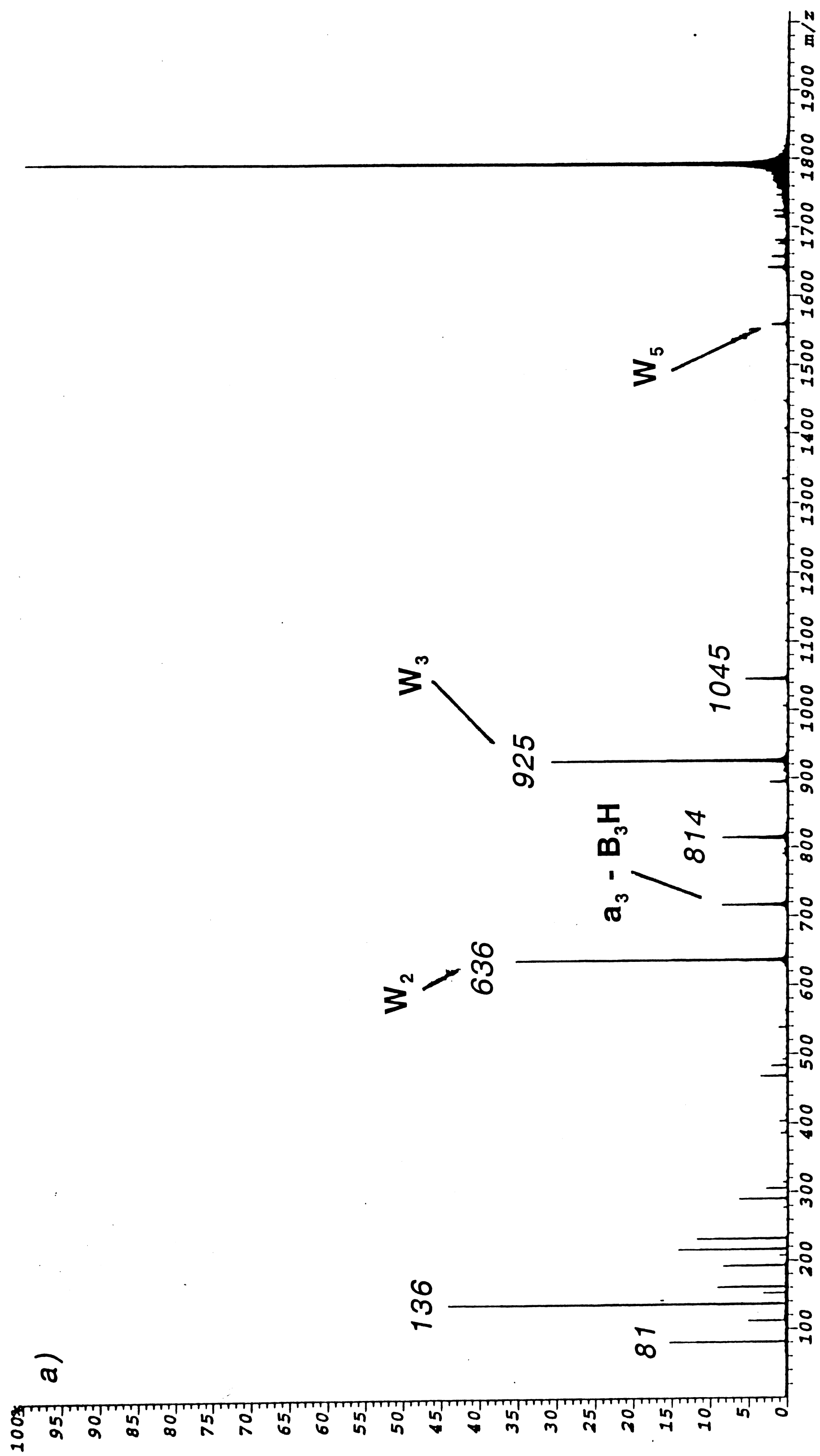

(continued on facing page)

Fig. 3. Tandem mass spectra of (a) $[M + H]^+$ ion (*m/z* 1791) and (b) $[M - H]^-$ ions of 5′-ATGCAT-3′ (*m/z* 1789).

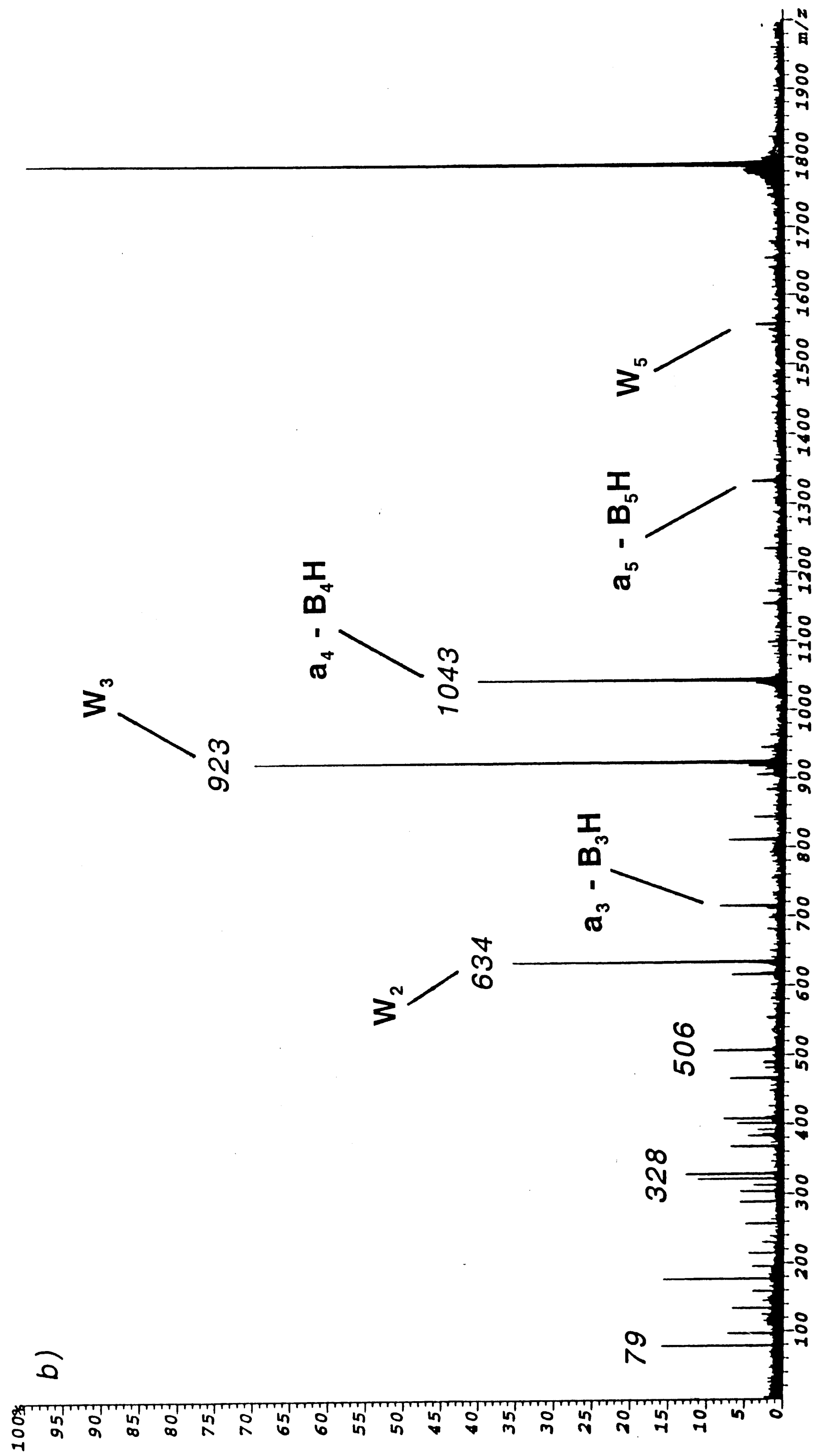

Fig. 3. *(continued)*

Table 4
Comparison of product ion spectra of $[M - 2H]^{2-}$ and $[M + 2H]^{2+}$ ions of 5′-d(CGTACG)-3′

m/z	Relative intensity (%)	Assignment	*m/z*	Relative intensity (%)	Assignment
1332.3	0.6	$[a_5 - B_5H - 2H]^-$			
1252.5	0.3	w_4^-	1254.5	0.5	$[w_4 + 2H]^+$
1019.4		$[a_4 - B_4H - 2H]^-$			
948.3	0.7	w_3^-			
894.7	100	$[M - 2H]^{2-}$	896.5	100	$[M + 2H]^{2+}$
839.2	1.1	$[M - CH - 2H]^{2-}$	841.4	4.8	$[M - CH + 2H]^{2+}$
827.1	0.6	$[M - AH - 2H]^{2-}$			
819.2	1.9	$[M - GH - 2H]^{2-}$	821.4	4.8	$[M - GH + 2H]^{2+}$
790.2	4.2	$[w_5 - 2H]^{2-}$	792.3	4.4	$[w_5 + 3H]^{2+}$
715.1	0.9	$[a_3 - B_3H - 2H]^-$	716.7	1.2	$[a_3 - B_3H]^+$
665.6	0.6	$[a_2 - B_2H - 2H]^-$			
635.1	5.4	w_2^-	636.9	0.2	$[w_2 + 2H]^+$
386.1	1.0	$[a_2 - B_2H - 2H]^-$	388.0	0.6	$[a_2 - B_2H]^+$
346.1	7.0	w_1^-	348.2	1.75	w_1^-
312.0	4.0	$[A_{nt} - H]^-$			
303.1	5.8	$[T_{nt} - H]^-$	305.1	0.5	$[T_{nt} + H]^+$
288.0	5.9	$[C_{nt} - H]^-$	290.1	6.3	$[C_{nt} + H]^+$
257.0	4.9	$[s + p + s - H_2O - H]^-$ or $[p + s + p - H]^-$			
230.0	2.8	$[sG - H_2O - H]^-$	232.1	3.0	$[sG - H_2O + H]^+$
214.0	4.7	$[sA - H_2O - H]^-$	216.1	7.9	$[sA - H_2O + H]^+$
195.0	4.2	$[s + p + H_2O - H]^-$			
			192.1	3.2	$[sC - H_2O + H]^+$
177.0	5.8	$[p + s - H]^-$			
158.9	4.1	$[s + p - H_2O - H]^-$	161.1	2.0	$[s + p - H_2O + H]^+$
150.0	1.3	G^-	152.1	39.8	$[GH_2]^+$
134.1	0.7	A^-	136.1	5.8	$[AH_2]^+$
125.0	1.3	T^-			
110.0	1.9	C^-	112.1	8.0	$[CH_2]^+$
96.9		$[s\text{-}H]^-$ or $[p + H_2O - H]^-$			
79.0	17.8	$[p - H]^-$ (PO_3^-)	81.1	9.5	$[s - H_2O + H]^+$

s = deoxyribose-H_2O ($C_5H_6O_2$), M_r = 98.0368 Da; p = PO_3H, M_r = 79.9663 Da; B_{nt} denotes a mononucleotide that may be either psB or sBp; $[(B_1...B_n)]$ denotes a polynucleotide that may be either $(psB_1...+psB_n)$ or $(sB_1p...+sB_np)$.
In some cases the major sequence ions may also be attributed to other sequence ions or internal fragments but for the sake of clarity these have been excluded from the table.

1043) and to a lesser extent $[a_3 - B_3H - 2H]^-$ (*m/z* 714). There is also a weak $[a_5 - B_5H - 2H]^-$ ion at *m/z* 1332. Of the base ions, A^- is the most abundant as was the case with the protonated precursors. There were some differences in the nature and relative abundance of the low mass product ions, with ions from the nucleotides $[X_{nt} + s - H]^-$ and $[X_{nt} + s + p - H]^-$ being of moderate abundance. These ions differed from those observed in the spectrum of the $[M + H]^+$ ion [Fig. 3(a)] and can be explained on the basis that the phosphate residues are the most probable sites of deprotonation.

Table 4 summarises the major product ions observed in the tandem mass spectra of doubly charged $[M + 2H]^{2+}$ [Fig. 2) and $[M - 2H]^{2-}$ (not shown) precursor ions of 5′-CGTACG-3′. The major difference between these spectra is in the relative abundance of the w_n sequence ions. These were $w_1 > w_2 > w_5$ (doubly charged) $> w_3 > w_4$ for the $[M - 2H]^{2-}$ precursor and $w_1 > w_5$ (doubly charged) $> w_4 > w_2$ for the $[M + 2H]^{2+}$ precursor. Thus loss of thymine as an anion to yield the singly charged w_3 sequence ion is evident in the spectrum of the $[M - 2H]^{2-}$ whereas this ion is not observed in the spectrum of the $[M + 2H]^{2+}$ ion. That the w_2 ion which arises from loss of A-4 is also of lower relative

abundance than the other sequence ions in the spectrum of the protonated precursor, is consistent with the lower proton affinity of A and/or the lower stability of protonated adenine as a leaving group.

As with the singly charged precursors, there are also some differences in the relative abundance of the low mass product ions in the tandem mass spectra of the doubly charged precursors. Whereas in the spectrum of the $[M + 2H]^{2+}$ ion, the BH_2^+ ions and $[s(base) - H_2O + H]^+$ ions are the most abundant, in the spectrum of the $[M - 2H]^{2-}$ ions the nucleotide and other products containing the phosphate residue (*m/z* 177, 195) are relatively more abundant than the base anions. Again, this is consistent with there being a difference in the location of the positive and negative charges in the oligonucleotides. One would expect the main sites of deprotonation to be the phosphate groups, whereas the main sites of protonation on the other hand are likely to be the nucleobases.

3.4. Tandem mass of fragment ions generated by in-source collisional activation

Tandem mass spectra were acquired for all of the product ions derived from 5′-CACGTG-3′ and 5′-CGTACG-3′ which were generated via collisional activation in the source using higher cone and skimmer voltages. The ions in each of the tandem mass spectra were assigned by first analysing the tandem mass spectra of the low *m/z* ions and then using these as a basis for interpreting the spectra of the higher *m/z* precursors. For example, Fig. 4 shows the tandem mass spectra of the source-generated fragment ions *m/z* 590, *m/z* 670, and *m/z* 781 derived from 5′-CACGTG-3′. The precursor ion of *m/z* 590 [Fig. 4(a)] is attributed to a string of three phosphate and two sugar residues (or vice versa less H_2O) containing an adenine base. The identities of the major fragment ions are given in Table 2. Similarly, the product ions in the spectrum of *m/z* 670 [Fig. 4(b)] indicate this ion comprises an adenine attached to a string of three phosphate and three sugar residues. Each of these product ions is present in the spectrum of the *m/z* 781 precursor [Fig. 4(c)] that aids in the assignment of this ion as a chain of three phosphate and three sugar residues plus adenine and cytosine. It should be noted, however, that it was not possible to determine the exact 5′-3′ structure of these types of fragment ions because the tandem mass spectra do not yield information concerning the points of cleavage along the phosphodiester backbone nor the specific sugar groups in the backbone "string" to which the bases are attached.

Table 5 shows the major ions observed in the tandem mass spectra of the in-source generated product ions. A number of trends are evident from the table. First, the $[base + (s - H_2O) + H]^+$ ions (*m/z* 216 for adenine and *m/z* 192 for cytosine) are relatively abundant in all the tandem mass spectra of the in-source precursors that include adenine and, to a lesser extent, cytosine. The corresponding ions from guanine (*m/z* 232) and thymine (*m/z* 207) are generally of low abundance or absent from these spectra. In the spectra of backbone ions containing adenine and one or more other bases, the *m/z* 216 ion is generally the most abundant. This ion was also one of, if not the, most abundant product ions in the tandem mass spectra of the intact oligonucleotides, suggesting this ion is particular stable. Similarly, *m/z* 81 (more below) was evident as an abundant product ion in the majority of spectra.

Fig. 5 shows the tandem mass spectra of *m/z* 81 and *m/z* 216 ions from in-source collisional activation of 5′-CGTACG-3′. There has been some disagreement regarding the assignment of this fragment ion because Wang et al. claims to give the first direct evidence that the ion at *m/z* 81 is $H_2PO_3^+$ [15]. Phillips and McCloskey, however, attribute the ion at *m/z* 81 to a fragment of the sugar based on the number of exchangeable hydrogens [17]. The tandem mass spectrum of the *m/z* 81 ion [Fig. 5(a)] shows product ions representative of the cleavage of a furan ring structure. The most abundant ion in the spectrum at *m/z* 27 may correspond to the ion $C_2H_3^+$. The ion at *m/z* 26 may be attributed to $C_2H_2^+$, and the ion at *m/z* 29 would seem to arise from HCO^+. The ion at *m/z* 53 may arise from loss of CO from the precursor ion, with the series of ions at *m/z* 52, *m/z* 51, and *m/z* 50, owing to the respective neutral losses of HCO, CH_2O, and CH_3O. The ion at *m/z* 39 corresponds to the

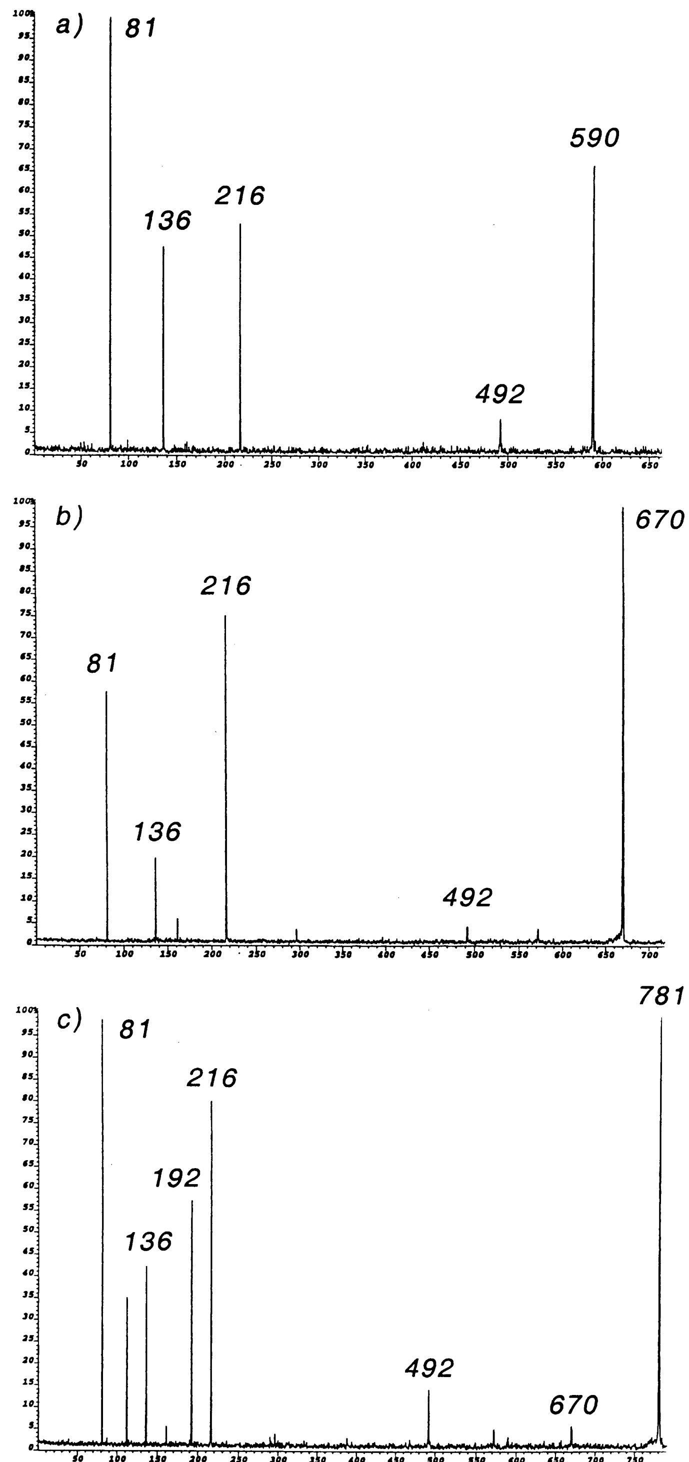

Fig. 4. Tandem mass spectra of product ions generated by in-source collisional activation of 5′-CACGTG-3′ (a) *m/z* 590, (b) *m/z* 670, and (c) *m/z* 781.

Table 5
Summary of tandem mass spectra of product ions of 5′-CACGTG-3′ and 5′-CGTACG-3′ generated by in-source collisional activation

5′-CACGTG-3′	Precursor ion (*m/z*)	Major product ions	Minor product ions
Loss of GH and H_2O	1623.3	192, 216, 492, 781, 990	81, 112, 136, 572, 590, 670, 812
$[w_5 - GH + 2H]^+$	1432.3	81, 152, 216, 492, 652, 981	112, 136, 192, 234, 830
$[a_4 - B_4H]^+$	990.0	81, 112, 136, 192, 216, 492, 590	670, 780
$[w_3 + 2H]^+$	981.1	81, 152	232, 483, 652, 830
$[a_4 - B_4H - AH]^+$	855.1	81, 112, 192	161, 388, 468
$[w_3 - GH + H]^+$	830.1	81, 136, 152	112, 136, 216, 232, 483, 510, 652
$[(GT) + p + s + H]^+$	812.1	232	81, 312
$[(AC) + p + s + H_2O + H]^+$	799.2	81, 112, 136, 216, 492	590
$[(AC) + p + s + H]^+$	780.9	81, 112, 136, 192, 216	161, 492, 572, 670
$[A_{nt} + s + p + s + p + s + H]^+$	768.1	81, 136, 216	
$[a_3 - B_3H]^+$	701.1	81, 136, 216, 492	112, 161, 192, 412, 510, 590
$[A_{nt} + p + s + p + s + H]^+$	670.1	81, 136, 216	161, 296, 492, 572
$[w_2 + 2H]^+$	652.0	81, 152	161, 216, 232, 296, 305, 385, 483
$[(AC) + H]^+$	603.1	81, 216	112
$[sA - H_2O + H]^+$	216.1	81	27, 53
5′-CGTACG-3′			
$[w_5 - GH + 2H]^+$	1432.3	81, 216, 796, 1253	305, 716, 894, 1005, 1085
$[c_5 - CH]^+$ or $[x_5 - GH]^+$	1414.2	81, 112, 136, 216, 796	112, 136, 161, 894, 1005
$[a_5 - B_5H]^+$	1334.8	81, 136, 216, 716, 796	
$[(TA) + p + s + p + s + H]^+$	974.0	81, 136, 216	796, 876
$[(TA) + s + p + s - H_2O + H]^+$	876.2	81, 216	136, 296
$[(TA) + s + H]^+$	715.7	81, 136	161, 216, 305, 385, 412, 483
$[w_2 + 2H]^+$	636.8	81, 112, 152	192, 348
$[C_{nt} + p + s + H]^+$	467.9	81, 192	112
$[w_1 + 2H]^+$	348.0	81, 152	
$[sG - H_2O + H]^+$	332.0	81, 152	
$[sC - H_2O + H]^+$	192.1	53, 81	27, 39, 42, 69, 112, 125

s = deoxyribose-H_2O ($C_5H_6O_2$), M_r = 98.0368 Da; p = PO_3H, M_r = 79.9663 Da; B_{nt} denotes a mononucleotide that may be either psB or sBp; $[(B_1 \ldots B_n)]$ denotes a polynucleotide that may be either ($psB_1 \ldots +psB_n$) or ($sB_1p \ldots +sB_np$).

In some cases the major sequence ions may also be attributed to other sequence ions or internal fragments but for the sake of clarity these have been excluded from the table; similarly ions of <2% relative intensity are also not included.

species $C_3H_3^+$ that would result from elimination of CH_2CO. The less abundant ions at *m/z* 38 and *m/z* 37 may arise from losses of the neutral species C_2H_3CO and C_2H_4CO, respectively. Therefore the fragmentation observed in the tandem mass spectrum of the product ion at *m/z* 81 strongly supports the fact that this is a sugar ion, with the furan structure proposed by Phillips and McCloskey, and therefore does not arise from a protonated phosphate, $H_2PO_3^+$. Further evidence that the *m/z* 81 ion is derived from the sugar residue is provided by the fact that this is the major product ion in the tandem mass spectrum of *m/z* 216, i.e. $[sA - H_2O + H]^+$ shown in Fig. 5(b), and in the tandem mass spectra of *m/z* 192 and *m/z* 232, which are the corresponding ions containing cytosine and guanine, respectively (see Table 5). In these examples, the ion at *m/z* 81 could not be derived from a phosphate residue without a substantial rearrangement of the base from the sugar to the phosphate in generating these precursor ions. That the *m/z* 81 fragment derived from the sugar is much more abundant than the ions derived from the base ion in each case contrasts with the results obtained in separate studies of nucleosides $[base + s + H]^+$ in which BH_2^+ ions were typically the major product ions [23]. This suggests that the charge is most probably located

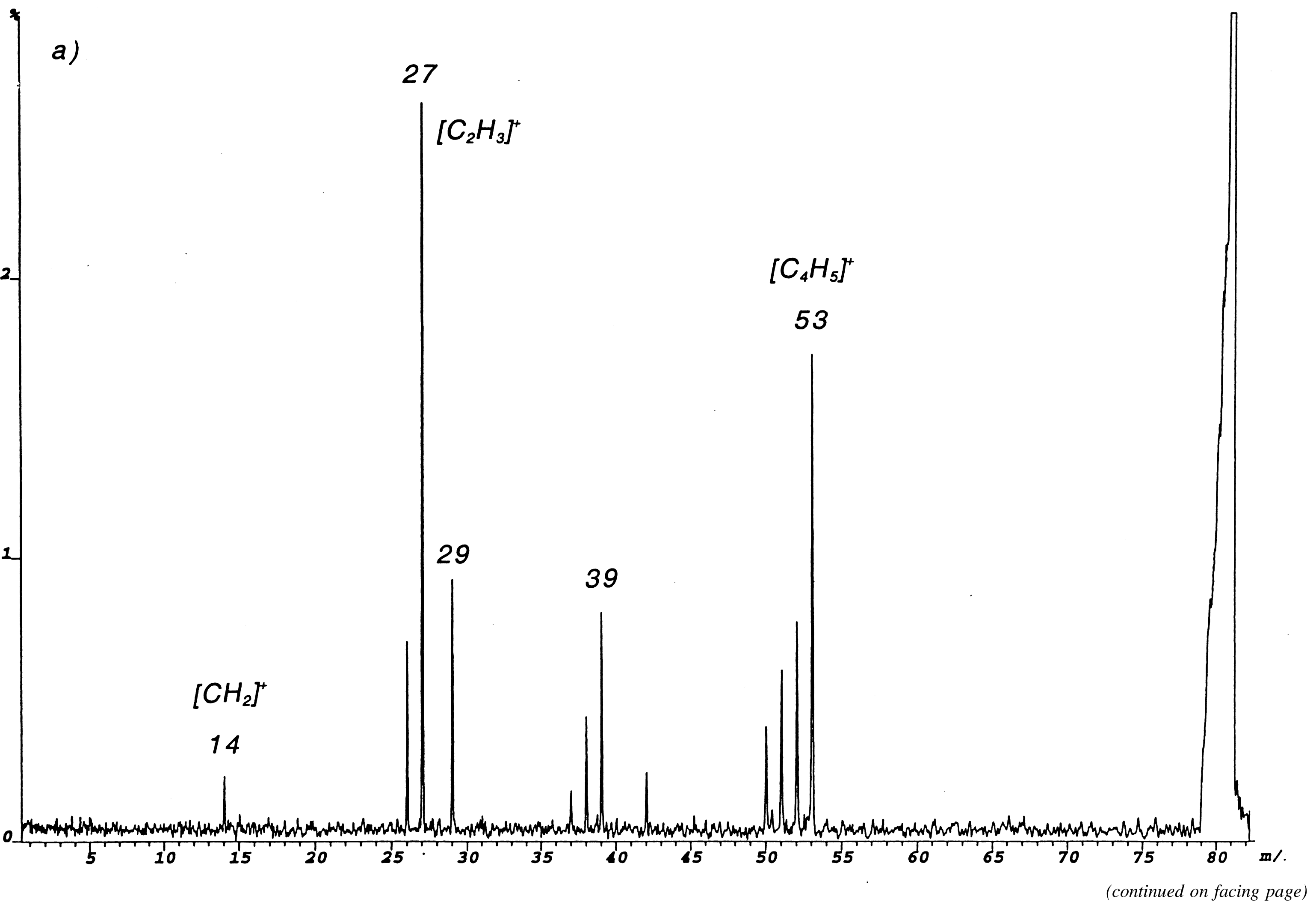

Fig. 5. Tandem mass spectra of product ions generated by in-source collisional activation of 5′-CGTACG-3′ (a) $[s - H_2O + H]^+$ *m/z* 81 and (b) $[sA - H_2O) + 2H]^+$ *m/z* 216.

(continued on facing page)

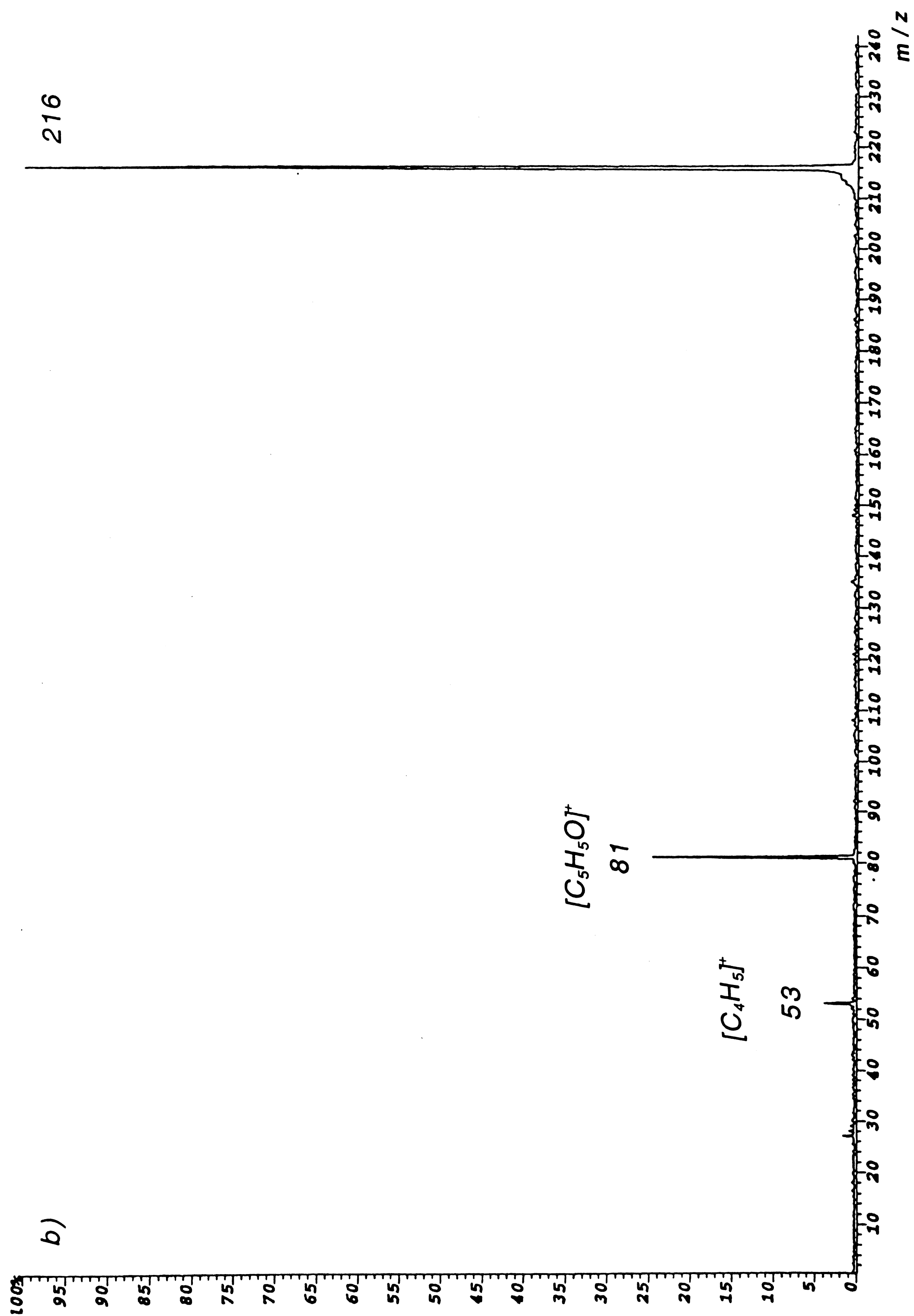

Fig. 5. *(continued)*

on the sugar residue in the former case and/or that the transfer of an additional proton from the unsaturated furan ring residue necessary to form the BH_2^+ ions is unfavourable.

4. Discussion

The tandem mass spectra of positively charged oligonucleotides obtained here showed some differences from those reported in previous work using triple quadrupoles, as might be expected given that the available collision energy is higher on the hybrid TOF instrument. First, the spectra do not show the same trends as those obtained on the triple quadrupoles, whereby the abundance of the protonated base BH_2^+ ions can be predicted based on the combined effect of the position of the base and the relative proton affinities of the bases, i.e. $G > C > A \gg T$. The only exception to this was that, consistent with all previous studies of protonated oligonucleotides, protonated thymine was never observed. Second, there were differences in the relative abundance of the base ions derived from singly and doubly charged precursors of the same oligonucleotide. This suggests that the charge of the precursor has a stronger influence on the abundance of ions from the bases than the position of the base. However, a larger number of sequences would need to be examined to establish this conclusively. The data for the singly charged ions contrasts with earlier studies of dinucleotides in which the BH_2^+ ion from the 3′ base is always the most abundant [17,18]. This may indicate that there is a higher probability of the internal bases being protonated in these larger oligonucleotides whereas in the dinucleotides there are only two possible sites of protonation (assuming only the bases are protonated).

A further significant difference between these data and the triple quadrupole studies is the observation of a significant number of fragment ions containing "strings of backbone," or chains of sugar and phosphate groups from which various bases had been lost (especially guanine and to a lesser extent cytosine). This was demonstrated by the tandem mass spectrum of the $[M + H]^+$ ion of 5′-CACGTG-3′ where a series of eight product ions are present owing to various additions of sugar and phosphate groups to the A mononucleotide. Another series of seven ions is observed where the strings of backbone incorporate the bases A and C as shown in Table 2. We were unable to postulate a mechanism to account for the formation of these ions, given that in many cases there were several possible structures with the same mass and the results of tandem mass spectrometry experiments on product ions formed in the source were not always definitive. However, since these types of "backbone ions" are not evident in high abundance in the tandem mass spectra of positively charged oligonucleotides obtained on triple quadrupole instruments, it is likely that these ions are formed via higher energy pathways (or over different time periods) than the w and a-B sequence ions.

The effect of charge location on positive ion oligonucleotide fragmentation also appears to play a major role in determining the types of "strings of backbone" ions observed in tandem mass spectra. Although the difference in proton affinities of A, C, and G nucleobases is not large, the greater propensity for C and G base loss can be explained on the basis of charge location of the various nucleobases. The greater stability of the N glycosidic bond in an A nucleoside in comparison to the C and G nucleosides could arise from the furan residue being protonated rather than the base on the A nucleoside. This hypothesis is supported by the fact that the $[A + s - H_2O + H]^+$ ions are significantly more abundant than the corresponding ions incorporating the other bases. Because the thymine has a very low probability of being protonated, the N-glycosidic bond between a sugar and thymine is not as susceptible to fragmentation and this could explain the series observed for 5′-CGTACG-3′. The fact that an analogous series incorporating only the thymine base does not appear could be a consequence of there being no available protonation site in that case, which prevents observation of these fragments in the positive ion mode.

The differences in relative abundance of sequence ions observed in positive ion tandem mass of oligonucleotides mostly reflect the influence of the loss of

thymine rather than the fact that the ions are positively charged per se because singly charged anions are similarly constrained with respect to loss of neutral thymine and the tandem mass spectra of the singly charged precursors (either protonated or deprotonated) are remarkably similar. In contrast, the spectra of multiply charged ions are very different because loss of thymine as an anion to generate singly charged sequence ions is possible for negatively charged precursors where $z \geq 2$. This is consistent with all previous studies of positive and negatively [3–12] charged oligonucleotides.

5. Conclusions

The high energy tandem mass spectra of protonated oligonucleotides show some similarities to the tandem mass spectra obtained on triple quadrupole instruments, however, the presence of additional product ions corresponding to strings of backbone ions and the relatively high abundance of low mass product ions (principally containing adenine) may complicate the spectra if they were to be used for sequencing. The trends with respect to formation of ions from loss of the nucleobases and the relative abundance of protonated base ions are also less straightforward than those reported previously, albeit the same "gaps" in the sequence ions when thymine is present are evident in the spectra shown here and the loss of neutral guanine and cytosine is clearly favourable. The tandem mass spectra of fragment ions generated by in-source collisional activation assisted in the assignment of the product ions; however, these spectra were also complicated by the mass redundancies between sugar and phosphate residues. One definitive example of the value of these experiments was the case of *m/z* 81, which we have shown here to be derived from the sugar, but which had previously been assigned in low energy tandem mass spectra to the protonated phosphate residue with the same nominal mass. Although it was not possible to derive fragmentation mechanisms to account for the formation of the backbone ions observed here, this could be the subject of further study by the choice of appropriately labeled oligonucleotides (e.g. using O^{18} labels of the phosphates) and/or by differentially labeling the termini.

Acknowledgements

Grants from the Australian Research Council, Ramaciotti Foundation, and the University of Wollongong that enabled the purchase of the electrospray mass spectrometer are gratefully acknowledged. The Australian Research Council supported this work. A.W. acknowledges the award of a postdoctoral fellowship from the Danish Natural Sciences Research Council.

References

[1] P.A. Limbach, P.F. Crain, J.A. McCloskey, Curr. Opin. Biotech. 6 (1995) 96.
[2] E. Nordhoff, F. Kirpekar, P. Roepstorff, Mass Spectrom. Rev. 15 (1996) 67.
[3] S.A. McLuckey, S. Habibi-Goudarzi, J. Am. Chem. Soc. 115 (1993) 12 085.
[4] S.A. McLuckey, G.J. Van Berkel, G.L. Glish, J. Am. Soc. Mass Spectrom. 3 (1992) 60.
[5] S.A. McLuckey, S. Habibi-Goudarzi, J. Am. Soc. Mass Spectrom. 5 (1994) 740.
[6] S.A. McLuckey, G.J. Van Berkel, D.E. Goeringer, G.L. Glish, Anal. Chem. 66 (1994) 689A.
[7] S.A. McLuckey, G. Vaidyanathan, S. Habibi-Goudarzi, J. Mass Spectrom. 30 (1995) 1222.
[8] S.A. McLuckey, G. Vaidyanathan, Int. J. Mass Spectrom. Ion Processes 162 (1997) 1.
[9] J. Ni, S.C. Pomerantz, J. Rozenski, Y. Zhang, J.A. McCloskey, Anal. Chem. 68 (1996) 1989.
[10] J. Ni, S.C. Pomerantz, J.A. McCloskey, Nucl. Acids Symp. Series 35 (1996) 113.
[11] M.G. Bartlett, J.A. McCloskey, S. Manalili, R.H. Griffey, J. Mass Spectrom. 31 (1996) 1277.
[12] J.P. Barry, P. Vouros, A. Van Schepdael, S.-J. Law, J. Mass Spectrom. 30 (1995) 993.
[13] K.A. Sannes-Lowery, D.P. Mack, P. Hu, H.Y. Mei, J. Am. Soc. Mass Spectrom. 8 (1997) 90.
[14] J. Ni, M.A. Mathews, J.A. McCloskey, Rapid Commun. Mass Spectrom. 11 (1997) 535.
[15] P. Wang, M.G. Bartlett, L.B. Martin, Rapid Commun. Mass Spectrom. 11 (1997) 846.
[16] (a) C.E. Costello, K.M. Comess, A.S. Plaziak, D.P. Bancroft, S.J. Lippard, Int. J. Mass Spectrom. Ion Processes 122 (1992) 255; (b) G. Lowe, J.A. McCloskey, J. Ni, T. Vilaivan, Biorg. Med. Chem. 4 (1996) 1007.
[17] D.R. Phillips, J.A. McCloskey, Int. J. Mass Spectrom. Ion Processes 128 (1993) 61.

[18] J. Boschenok, M.M. Sheil, Rapid Commun. Mass Spectrom. 10 (1996) 144.
[19] M.T. Rodgers, S. Campbell, E.M. Marzluff, J.L. Beauchamp, Int. J. Mass Spectrom. Ion Processes 148 (1995) 1.
[20] G. Wickham, P. Iannitti, J. Boschenok, M.M. Sheil, Rapid Commun. Mass Spectrom. 9 (1995) S197.
[21] R.H. Bateman, M.R. Green, G. Scott, E. Clayton, Rapid Commun. Mass Spectrom. 9 (1995) 1227.
[22] D.M. Reddy, C.R. Iden, Nucleos. Nucleot. 12 (1993) 815.
[23] F.W. Crow, K.B. Tomer, M.L. Gross, J.A. McCloskey, D.E. Bergstrom, Anal. Chem. 139 (1984) 243.